BBA - Molecular Basis of Disease 1865 (2019) 1226–1240

Contents lists available at ScienceDirect

BBA - Molecular Basis of Disease

journal homepage: www.elsevier.com/locate/bbadis

Downregulated lncRNA-MIAT confers protection against erectile dysfunction by downregulating lipoprotein lipase *via* activation of miR-328a-5p in diabetic rats

Wei Huo, Yi Hou, Yang Li, Hai Li*

Department of Urology, China-Japan Union Hospital of Jilin University, Changchun 130021, PR China

ARTICLE INFO

Keywords:
Diabetes
Erectile dysfunction
microRNA-328a-5p
Long noncoding RNA myocardial infarction-associated transcript
Lipoprotein lipase
Smooth muscle cells
Endothelial cells

ABSTRACT

Erectile dysfunction (ED) is a common comorbidity in males with diabetes. In this study, we aimed to investigate how lncRNA-MIAT affects ED in diabetes and the involved mechanism. Microarray analysis was performed to screen ED-related differentially expressed genes, regulatory microRNA (miR) and long noncoding RNA (lncRNA). Highly expressed lipoprotein lipase (LPL) was identified, and subsequently miR-328a-5p and lncRNA-MIAT were determined. Diabetes was induced by streptozotocin in rats, and diabetic rats with ED were selected. Vascular smooth muscle cells (VSMCs) and vascular endothelial cells (VECs) were cocultured. The siRNA against lncRNA-MIAT, miR-328a-5p mimic and overexpression vector of LPL were transfected to investigate the specific effects of miR-328a-5p, lncRNA-MIAT and LPL on ED in diabetes. The expression of LPL, lncRNA-MIAT and miR-328a-5p in the serum of diabetic patients was measured. Increased LPL and lncRNA-MIAT and reduced miR-328a-5p were observed in diabetic patients. In addition, ED led to upregulated LPL and lncRNA-MIAT and downregulated miR-328a-5p in serum of diabetic patients and VSMCs of diabetic rats, especially in those with ED. LncRNA-MIAT directly regulated miR-328a-5p, which directly targeted LPL. LncRNA-MIAT upregulated LPL by acting as a ceRNA of miR-328a-5p. Silencing of lncRNA-MIAT and LPL or miR-328a-5p overexpression reduced VEC apoptosis and increased cell proliferation. In addition, an increased intracavernosal pressure (ICP)/mean arterial pressure (MAP) ratio was noted in the corpus cavernosum of rats and inhibited VEC injury. Taken together, our data demonstrated that depleted lncRNA-MIAT suppressed LPL by increasing miR-328a-5p, thereby inhibiting VEC injury to attenuate ED in diabetic rats.

1. Introduction

Diabetes is defined as a metabolic disorder of multiple etiologies characterized by chronic hyperglycemia and typically causes the shortage of insulin secretion or defects in the insulin action and sometimes even both of them [1]. Diabetes is also reported as a cause for the development of erectile dysfunction (ED) [2], which leads to a consistent or recurrent inability of the male to attain or maintain penile erection sufficient for sexual intercourse. ED exhibits 71% prevalence in men with diabetes and prevalently occurs within 10 years after diabetes diagnosis [3,4]. Despite some improvement in pharmacotherapeutic approaches in this field, ED is still difficult to treat medically [5]. A study demonstrated that the expression of some microRNAs (miRNAs) could be used as useful biomarkers for the early diagnosis of ED in patients with diabetes, such as miR-93, miR-320 and miR-16 [6] Therefore, a better understanding of molecular mechanism of miRNAs in ED will be beneficial for the development of ED treatments.

Long noncoding RNA myocardial infarction associated transcript (lncRNA-MIAT) is expressed in endothelial cells and mediates various endothelial functions, including vascular sprouting and migration [7]. A recent study demonstrated that the amount of lncRNA-MIAT is significantly increased in diabetic retinas and endothelial cells that were cultured in high-glucose medium, and the deletion of MIAT ameliorates retinal microvascular dysfunction resulting from diabetes and inhibits endothelial cell proliferation, migration, and tube formation [7]. A search for the interactors of lncRNA-MIAT using the online website microRNA.org predicted a direct interaction between lncRNA-MIAT and miR-328a-5p. MiRNAs are small noncoding RNAs that participate in posttranscriptional gene regulation in plants and animals [8]. The overexpression of miR-328 improves glucose tolerance and insulin

* Corresponding author at: Department of Urology, China-Japan Union Hospital of Jilin University, Changchun 130021, No. 126, Xiantai Street, Jilin Province, PR China.
E-mail address: lihai@jlu.edu.cn (H. Li).

https://doi.org/10.1016/j.bbadis.2019.01.018
Received 14 August 2018; Received in revised form 13 December 2018; Accepted 15 January 2019
Available online 17 January 2019

sensitivity in mice with type 2 diabetes mellitus [9]. However, another recent study revealed significant upregulation of miR-328a in the corpus cavernosum of obese rats with ED, which subsequently impaired erectile function in rats [10]. In addition, the website microRNA.org also predicted that miR-328a-5p could bind to the 3′untranslated region (UTR) of lipoprotein lipase (LPL), which is a serine hydrolase that secretes free fatty acids (FFAs) from circulating triglyceride (TG)-rich lipoproteins. LPL is a contributor to FFA-mediated signaling in the brain, and its deficiency in neurons modifies the regulation of energy balance and subsequently results in obesity [11]. Furthermore, it has been revealed that LPL mRNA and protein levels are increased in type 2 diabetes [12]. In a previous study, highly expressed LPL accelerates the development of ED [13]. Here, we seek to investigate the expression of lncRNA-MIAT, LPL and miR-328a-5p in streptozotocin (STZ)-induced diabetic rats with ED and examine vascular endothelial cell (VEC) injury *in vitro* when endogenous expression of lncRNA-MIAT and miR-328a-5p were affected.

2. Results

2.1. Highly expressed lncRNA-MIAT and LPL but lowly expressed miR-328a-5p are observed in diabetic ED

To identify some mRNAs that are potentially linked to ED, we performed bioinformatics prediction based on the chip data GSE2457. We screened differentially expressed genes (DEGs) with *P*-value < 0.05 and |LogFoldChange| > 2 and generated a heat map for the top 10 DEGs (Fig. 1A) that exhibited largest gene expression difference. Then, we applied these DEGs in subsequent analysis of gene association. According to the protein intersection among the first 10 DEGs from the String database, a PPI network was subsequently constructed (Fig. 1B), in which the LPL gene interacted with several DEGs. These findings indicate that LPL potentially has a vital effect on diabetic ED. Based on miRWalk retrieval results, 466 miRNAs were identified that target LPL. To determine which miRNA was most likely to regulate LPL, we screen

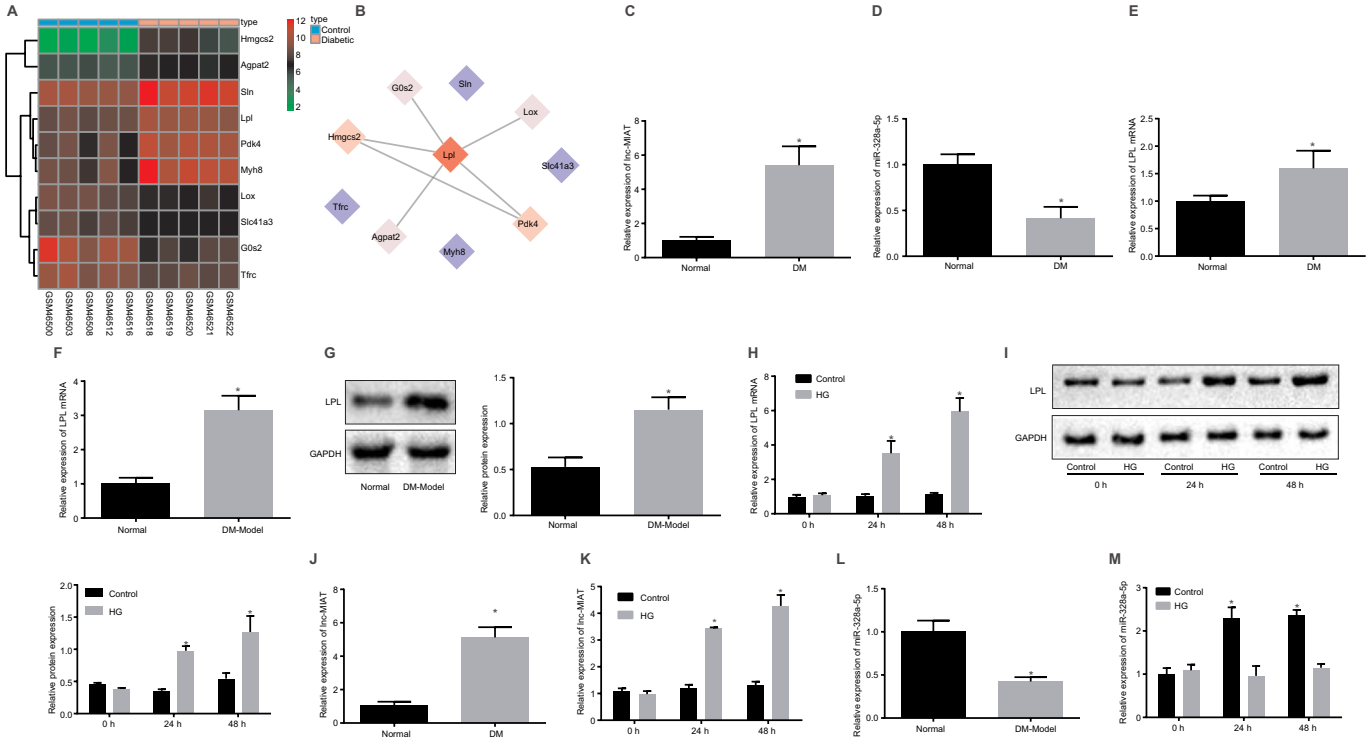

Fig. 1. Significant increase in lncRNA-MIAT and LPL expression and decrease in miR-328a-5p expression are observed in diabetic ED. A, Heat map of the first 10 DEGs from GSE2457 chip data; abscissa represents the sample number, ordinate represents the DEGs, the diagram in the upper right represents color gradation, each rectangle in the map corresponds to a sample expression value; B, PPI network of DEGs in diabetic ED; C–E, the expression of lncRNA-MIAT, miR-328a-5p and LPL in diabetic patients with ED and healthy individuals examined by qRT-PCR, $*p < 0.05$, *vs.* normal group, normal control of healthy individuals = 40 and DM patients = 58; F, LPL mRNA expression in diabetic rats with ED and normal rats examined by qRT-PCR, $*p < 0.05$, *vs.* normal group, normal rats = 8 and DM rat models = 48; G, protein bands and levels of LPL in diabetic rats with ED and normal rats examined by western blot analysis, $*p < 0.05$, *vs.* normal group, normal rats = 8 and DM rat models = 48; H, LPL mRNA levels in VSMCs cultured in high-glucose medium and normal medium examined by qRT-PCR, $*p < 0.05$, *vs.* control group; I, the protein bands and levels of LPL in VSMCs cultured in high-glucose medium and normal medium examined by western blot analysis, $*p < 0.05$, *vs.* control group; measurement data were expressed as the mean ± standard deviation, comparison between two groups was analyzed using *t*-test, and the data in Panel H and Panel I were compared using two-way analysis of variance; the experiment was repeated thrice; J, lncRNA-MIAT levels in diabetic rats with ED and normal rats examined by qRT-PCR, normal rats = 8, DM rat models = 48, $*p < 0.05$, *vs.* normal group; K, lncRNA-MIAT levels in VSMCs cultured in high-glucose medium and normal medium examined by qRT-PCR, $*p < 0.05$, *vs.* control group; measurement data were expressed as the mean ± standard deviation, comparison between two groups was analyzed using *t*-test, and the data in Panel K were analyzed using two-way analysis of variance; the experiment was repeated thrice; L, miR-328a-5p expression in diabetic rats with ED and normal rats examined by qRT-PCR, normal rats = 8, DM rat models = 48, $*p < 0.05$, *vs.* normal group; M. miR-328a-5p expression in VSMCs cultured in high-glucose medium and normal medium examined by qRT-PCR, $*p < 0.05$, *vs.* control group; measurement data were expressed as the mean ± standard deviation, comparison between two groups was analyzed using *t*-test, and the data in Panel M were analyzed using two-way analysis of variance; the experiment was repeated thrice; lncRNA-MIAT, long noncoding RNA myocardial infarction associated transcript; LPL, lipoprotein lipase; miR-328a-5p, microRNA-328a-5p; ED, erectile dysfunction; DEGs, differentially expressed genes; qRT-PCR, reverse-transcription quantitative polymerase chain reaction; VSMCs, vascular smooth muscle cells; PPI, protein-protein interaction; DM, diabetes mellitus.

Table 1
Primer sequence for qRT-PCR.

Gene	Sequence
LncRNA-MIAT	F: 5′-TCCCATTCCCGGAAGCTAGA-3′ R: 5′-GAGGCATGAAATCACCCCCA-3′
LPL	F: 5′-CCTGATGACGCTGATTTTGT-3′ R: 5′-AGGCAAGCTGGTGAGGATCTG-3′
miR-328a-5p	F: 5′-ACGGAAGGGCAGAGAGGGCCAG-3′ R: 5′-TGCCAGAAGGAGCACTTAGG-3′
eNOS	F: 5′-CCAGCTAGCCAAAGTCACCAT-3′ R: 5′-GTCTCGGAGCCATACAGGATT-3′
U6	F: 5′-TGCGGGTGCTCGCTTCGGCAGC-3′ R: 5′-CCAGTGCAGGGTCCGAGGT-3′
GAPDH	F: 5′-ACCACAGTAAATGCCATCAC-3′ R: 5′-TCCACCACCCTGTTGCTGTA-3′

Note: qRT-PCR, reverse-transcription quantitative polymerase chain reaction; F, forward; R, reverse; LncRNA-MIAT, long non-coding RNA myocardial infarction associated transcript; LPL, lipoprotein lipase, eNOS, endothelial nitric-oxide synthase; GAPDH, glyceraldehyde-3-phosphate dehydrogenase.

the predicted miRNAs with setting a screening criteria that "binding probability > 0.9, energy ≤30" as a condition, and then 3 miRNAs (miR-328a-5p, miR-1224 and miR-3593-5p) were identified. Given that miR-328 participates in cell injury induced by high glucose [9], we focused on the function of miR-328a-5p in LPL in diabetic ED. LncRNA-MIAT has been is highly expressed in diabetic animal models and affected diabetes and its pathological changes [7,14]. RNA22 prediction results revealed that lncRNA-MIAT might bind to miR-328a-5p (Fig. 1D). Combined with the bioinformatics prediction results, we hypothesized that lncRNA-MIAT might influence LPL *via* its combination with miR-328a-5p in diabetic ED. Additionally, quantitative reverse-transcription polymerase chain reaction (qRT-PCR) was applied to examine the expression of lncRNA-MIAT, miR-328a-5p and LPL. The results showed that the DM patients exhibited increased mRNA expression of lncRNA-MIAT and LPL but reduced miR-328a-5p expression compared with normal patients ($p < 0.05$) (Fig. 1C–E). qRT-PCR and western blot analysis were used to detect the mRNA and protein levels, respectively, of LPL in primary vascular smooth muscle cells (VSMCs) cultured in normal medium and high-glucose medium, and the results (Fig. 1F&G) showed that LPL mRNA and protein levels in VSMCs cultured in high-glucose medium were significantly increased compared with that cultured in normal medium ($p < 0.05$). Compared with normal rats, LPL mRNA and protein levels in the diabetes rats were also significantly increased ($p < 0.05$) (Fig. 1H&I, Supplementary Fig. 2C). A STZ-induced rat diabetes model was established to screen diabetic rats with ED using apomorphine (APO) to detect the expression of lncRNA-MIAT and miR-328a-5p in ED rats and normal rats. The results showed that lncRNA-MIAT expression in smooth muscle of penis of ED rats was significantly increased, whereas miR-328a-5p expression was reduced compared with that in normal rats ($p < 0.05$) (Fig. 1L).

To determine the expression of lncRNA-MIAT and miR-328a-5p in ED, VSMCs of penis were isolated and cultured with normal medium and high-glucose medium. The results (Fig. 1K&M, Supplementary Fig. 2A&B) revealed that lncRNA-MIAT expression was significantly increased, whereas miR-328a-5p expression was reduced in high-glucose medium ($p < 0.05$). In contrast, lncRNA-MIAT and miR-328a-5p expression revealed no obvious differences in cells cultured with normal medium ($p > 0.05$) (see Table 1).

Based on the above findings, we concluded that lncRNA-MIAT and LPL were upregulated in the smooth muscle of penis, whereas miR-328a-5p was downregulated in diabetic ED rats.

2.2. High-glucose triggers VEC injury

Vascular endothelial cells (VECs) cultured in normal medium and high-glucose medium were collected for assessment reactive oxygen species (ROS) levels, nitric oxide (NO) concentration and glutathione (GSH) content. Compared with VECs cultured in normal medium, ROS levels in VECs cultured in high-glucose medium were significantly increased, whereas NO and GSH levels as well as endothelial nitric-oxide synthase (eNOS) mRNA and protein levels were significantly decreased (all $p < 0.05$) (Table 2, Fig. 2A&B). The proliferation of VECs cultured in high-glucose medium was reduced, but the apoptosis rate was elevated. In addition, cleaved caspase-3 and Bax protein levels were significantly increased in VECs cultured in high-glucose medium (all $p < 0.05$) (Fig. 2C∼E). This finding suggests that metabolites produced by VSMCs under high-glucose medium could inhibit VECs and promote cell apoptosis.

Table 2
Serum levels of ROS, NO and GSH in VECs cultured in normal control medium and high-glucose medium.

	Control	Hypertonic control	HG
ROS (U/mL)	158.28 ± 10.71	153.77 ± 6.63	274.15 ± 10.51*
NO (uM)	95.47 ± 6.46	93.32 ± 4.46	74.51 ± 5.12*
GSH (nmol/mg protein)	60.10 ± 8.41	62.65 ± 2.65	36.36 ± 4.03*

Note: ROS, reactive oxygen species; NO, nitric oxide; GSH, glutathione; HG, high glucose; VECs, vascular endothelial cells; *$p < 0.05$, *vs*. the control group; the measurement data were expressed as mean ± standard deviation, and data between two groups were compared with *t*-test; the experiment was repeated 3 times.

2.3. Overexpressed lncRNA-MIAT/LPL induces VECs injury and promotes VECs apoptosis

After VSMCs were transfected with overexpressed lncRNA-MIAT, qRT-PCR and western blot analysis were performed to detect LPL mRNA and protein levels, respectively, in VSMCs. The results (Fig. 3A&B) showed that compared with the negative control (NC) group, LPL mRNA and protein levels were remarkably increased in the oe-lncRNA-MIAT group ($p < 0.05$). Subsequently, VSMCs overexpressing lncRNA-MIAT were co-cultured with VECs for 72 h, and LPL protein levels in VECs were remarkably increased in the oe-lncRNA-MIAT group compared with the NC group (Fig. 3C) (all $p < 0.05$). The results above indicated that lncRNA-MIAT overexpression increased LPL expression. Moreover, LPL in VSMCs induced by overexpression of lncRNA-MIAT accumulates in VECs.

Subsequently, VSMCs and VECs overexpressing lncRNA-MIAT or LPL were co-cultured in normal medium for 72 h, and then VEC injury indexes were detected. Compared with the NC group, ROS levels in the oe-lncRNA-MIAT and oe-LPL groups in VECs was significantly increased, and NO and GSH levels as well as eNOS mRNA and protein levels were significantly decreased (all $p < 0.05$). Compared with the oe-lncRNA-MIAT and oe-LPL groups, ROS levels in VECs were significantly increased, and NO and GSH levels as well as eNOS mRNA and protein levels were significantly reduced in the oe-lncRNA-MIAT + oe-LPL group (all $p < 0.05$) (Table 3, Fig. 3D&E).

Cell counting kit-8 (CCK-8) assay and flow cytometry were then used to measure cell proliferation and apoptosis rates (Fig. 3F∼H). Compared with the NC group, VEC proliferation was significantly reduced, whereas the apoptosis rate as well as cleaved caspase-3 and Bax expression were obviously increased in the oe-lncRNA-MIAT and oe-LPL groups (all $p < 0.05$). Compared with the oe-lncRNA-MIAT and oe-LPL groups, VEC proliferation was decreased, whereas the apoptosis rate as well as cleaved caspase-3 and Bax expression were significantly increased in the oe-lncRNA-MIAT + oe-LPL group (all $p < 0.05$). Based on the above results, we conclude that lncRNA-MIAT overexpression or LPL overexpression in normal medium could result in VEC injury and promote apoptosis.

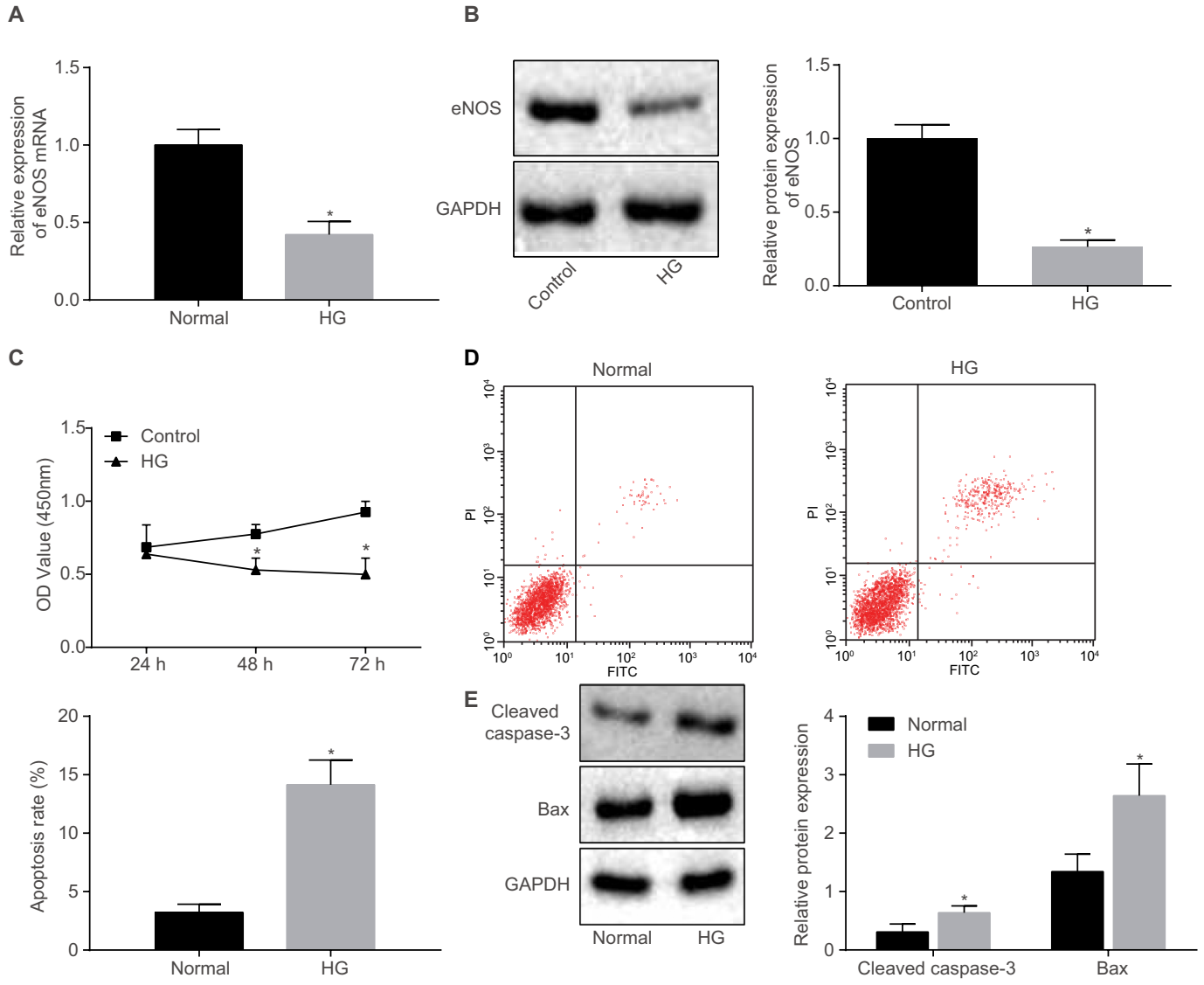

Fig. 2. High-glucose leads to VEC injury. A, qRT-PCR revealed that high-glucose led to reduction of eNOS mRNA levels in VECs; B, high glucose suppressed eNOS protein expression detected by western blot analysis; C, high glucose reduced VEC proliferation as measured by CCK-8 assay; D, high glucose increased VEC apoptosis rate as measured by flow cytometry; E, high glucose increased cleaved caspase-3 and Bax protein levels as detected by western blot analysis; *$p < 0.05$, *vs.* the control group; the measurement data were expressed as the mean ± standard deviation, and data between two groups were compared using *t*-test; data in Panel C were compared using two-way analysis of variance; the experiment was repeated thrice; lncRNA-MIAT, long noncoding RNA myocardial infarction associated transcript; LPL, lipoprotein lipase; miR-328a-5p, microRNA-328a-5p; ED, erectile dysfunction; VEC, vascular endothelial cells; qRT-PCR, reverse-transcription quantitative polymerase chain reaction; CCK-8, cell counting kit-8; eNOS, endothelial nitric-oxide synthase.

2.4. Downregulation of lncRNA-MIAT/LPL alleviates VECs injury and suppresses VECs apoptosis

After VSMCs were transfected with lncRNA-MIAT siRNA or LPL siRNA, qRT-PCR and western blot analysis were followed to detect LPL mRNA and protein levels, respectively, in VSMCs, and the results are presented in Fig. 4A&B. Compared with the si-NC group, LPL mRNA and protein levels in VSMCs were significantly reduced in the si-lncRNA-MIAT group ($p < 0.05$). Subsequently, VSMCs treated with lncRNA-MIAT siRNA or LPL siRNA were co-cultured with VECs for 72 h, and then LPL protein levels in VECs were detected. The results are shown in Fig. 4C. Compared with the si-NC group, LPL protein levels in VECs were significantly reduced in the si-lncRNA-MIAT and si-LPL groups (all $p < 0.05$) (Fig. 4C). LPL protein levels in VECs were also significantly reduced in the si-lncRNA-MIAT + oe-LPL group compared with the si-lncRNA-MIAT group ($p < 0.05$) (Fig. 4C).

After 48-h transfection, VSMCs and VECs were co-cultured in high-glucose medium for 72 h to detect VEC injury indexes. Compared with the si-NC group, ROS levels in VECs in the si-lncRNA-MIAT and si-LPL groups were strongly decreased, but NO and GSH levels as well as eNOS mRNA and protein levels were increased (all $p < 0.05$). Compared with the si-lncRNA-MIAT group, ROS levels in VECs were significantly increased, and NO and GSH levels as well as eNOS mRNA and protein levels were significantly reduced in the si-lncRNA-MIAT + oe-LPL group (all $p < 0.05$) (Table 4, Fig. 4D&E). CCK-8 assay and flow cytometry were used to measure cell proliferation and apoptosis rates (Fig. 4F~H). Compared with the si-NC group, VEC proliferation increased, whereas the apoptosis rate as well as cleaved caspase-3 and Bax expression were significantly decreased in the si-lncRNA-MIAT and si-LPL groups (all $p < 0.05$). Compared with the si-lncRNA-MIAT group, VEC proliferation decreased, whereas apoptosis rate as well as cleaved caspase-3 and Bax expression significantly increased in the si-

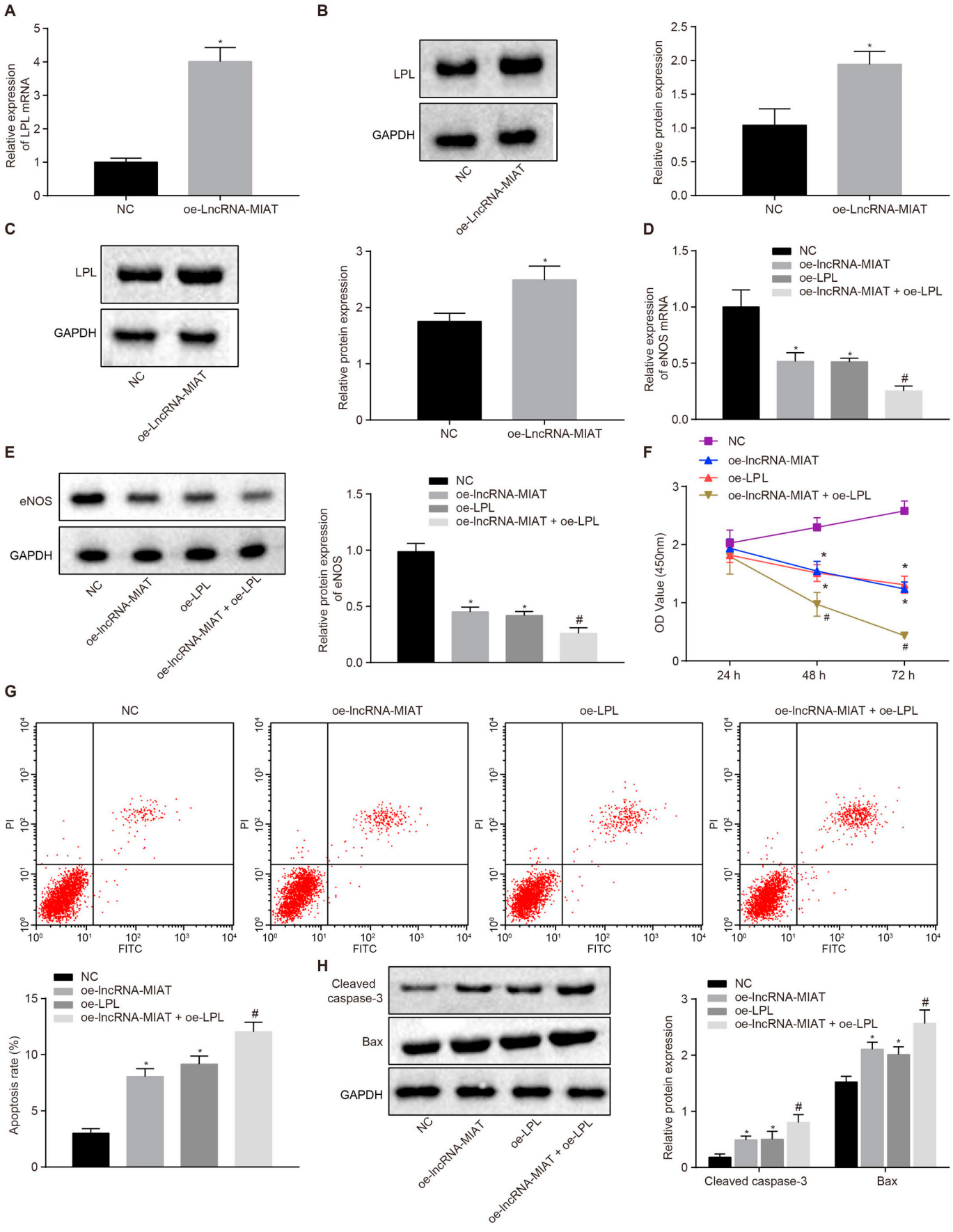

(caption on next page)

Fig. 3. Overexpression of lncRNA-MIAT or LPL leads to VEC injury. A, qRT-PCR revealed that lncRNA-MIAT overexpression induced LPL mRNA expression in smooth muscle; B, western blot analysis demonstrated that lncRNA-MIAT overexpression induced LPL protein levels in smooth muscle; C, western blot analysis demonstrated that lncRNA-MIAT overexpression increased LPL protein levels in VECs; D, qRT-PCR revealed that lncRNA-MIAT overexpression or LPL overexpression upregulated eNOS mRNA level in VECs; E, western blot analysis demonstrated that lncRNA-MIAT overexpression or LPL overexpression reduced the production of eNOS protein in VECs; F, lncRNA-MIAT overexpression or LPL overexpression decreased VEC proliferation, measured by CCK-8 assay; G, lncRNA-MIAT overexpression or LPL overexpression increased VEC apoptosis rate, measured by flow cytometry; H, lncRNA-MIAT overexpression or LPL overexpression increased cleaved caspase-3 and Bax protein levels, detected by western blot analysis; $^{*}p < 0.05$, *vs.* the NC group; $\#p < 0.05$, *vs.* the oe-lncRNA-MIAT and oe-LPL groups; the measurement data were expressed as the mean ± standard deviation, and comparisons among multiple groups were analyzed by one-way analysis of variance; data in Panel F were analyzed using two-way analysis of variance; the experiment was repeated thrice; lncRNA-MIAT, long noncoding RNA myocardial infarction associated transcript; LPL, lipoprotein lipase; miR-328a-5p, microRNA-328a-5p; ED, erectile dysfunction; NC, negative control; VEC, vascular endothelial cells; qRT-PCR, reverse-transcription quantitative polymerase chain reaction; eNOS, endothelial nitric-oxide synthase.

lncRNA-MIAT + oe-LPL group (all $p < 0.05$). The results above indicated that inhibition of lncRNA-MIAT or LPL might alleviate VEC injury induced by high glucose and hinder VEC apoptosis.

2.5. LncRNA-MIAT regulates LPL by competitively binding to miR-328a-5p

Fluorescence *in situ* hybridization (FISH) was performed to identify the location of lncRNA-MIAT in VSMCs. The results in Fig. 5A demonstrate that lncRNA-MIAT was mainly expressed in the cytoplasm and minimally expressed in nucleus. The green color represents lncRNA-MIAT, and blue marks nuclei. Given that lncRNA-MIAT was located in the cytoplasm and affects LPL expression, we hypothesized that lncRNA-MIAT functioned through acting as a ceRNA. To verify our hypothesis, we analyzed miRNA combined with lncRNA-MIAT and LPL and observed miR-328a-5p. We performed qRT-PCR to detect miR-328a-5p expression in smooth muscle and primary VSMCs cultured in high-glucose medium (Fig. 5B&C). Compared with the normal rats, miR-328a-5p expression was significantly reduced in the smooth muscle of penis in diabetic rats (all $p < 0.05$). Moreover, after 24-h and 48-h culture in high-glucose medium, miR-328a-5p expression was significantly reduced, compared with normal medium (all $p < 0.05$).

Using the online prediction website microRNA.org, we identified a binding site between lncRNA-MIAT and miR-328a-5p that was later verified *via* dual-luciferase reporter gene assay (Fig. 5D). Compared with the NC group, luciferase activity was significantly reduced in the lncRNA-MIAT-Wt group ($p < 0.05$), whereas luciferase activity was not altered in the lncRNA-MIAT-Mut group ($p > 0.05$). These results indicate that lncRNA-MIAT specifically binds to miR-328a-5p. RNA immunoprecipitation (RIP) results presented in Fig. 5F also demonstrated that lncRNA-MIAT bound to AGO2 protein, and lncRNA-MIAT is capable of targeting miR-328a-5p.

Online software prediction indicated that the binding site was located between miR-328a-5p and LPL-3'UTR (Fig. 5E). Thus, an LPL 3'UTR gene fragment was designed and synthetized. Using luciferase assays, luciferase activity was significantly reduced in the LPL-Wt group compared with the NC group ($p < 0.05$), whereas luciferase activity was not altered in the LPL-Mut group ($p > 0.05$). These results demonstrated that miR-328a-5p specifically binds to LPL.

qRT-PCR and western blot analysis were conducted to detect LPL mRNA and protein levels, respectively, when overexpressing or silencing lncRNA-MIAT and miR-328a-5p. The results (Fig. 5G&H) indicated that miR-328a-5p expression was reduced, whereas LPL mRNA and protein levels were significantly increased in the lncRNA-MIAT group compared with the oe-NC group ($p < 0.05$). Compared with the mimic-NC group, miR-328a-5p expression was increased, whereas LPL mRNA and protein levels were significantly reduced in the miR-328a-5p mimic group (all $p < 0.05$). The above results implied that lncRNA-MIAT might regulate LPL expression by acting as a ceRNA of miR-328a-5p.

2.6. Upregulation of miR-328a-5p or silencing lncRNA-MIAT alleviates ED in diabetic rats

We constructed an ED model to assess lentivirus transfection and inhibitor injection as well as detection of erectile frequency and intracavernosal pressure (ICP)/mean arterial pressure (MAP) ratio to investigate the function of miR-328-5p and lncRNA-MIAT in ED in diabetic rats. As shown in Fig. 6A&B and Supplementary Fig. 4, erectile frequency and ICP/MAP were significantly reduced in the ED group compared the normal group (all $p < 0.05$). No significant differences were observed in erectile frequency and ICP/MAP in the si-NC and mimic-NC groups (all $p > 0.05$). Erectile frequency and ICP/MAP were significantly increased in the si-lncRNA-MIAT group compared with the si-NC group (all $p < 0.05$). Compared with the mimic-NC group, erectile frequency and ICP/MAP were increased in the miR-328a-5p mimic group (all $p < 0.05$). Reduced erectile frequency and ICP/MAP were observed in the miR-328a-5p mimic + oe-LPL group compared with the miR-328a-5p mimic group (all $p < 0.05$). These findings suggested that silencing lncRNA-MIAT or overexpressing miR-328a-5p could benefit patients with diabetic ED. In contrast, LPL upregulation reverses the alleviation of ED mediated by miR-328a-5p.

To further identify the role of lncRNA-MIAT and miR-328a-5p in VEC injury in corpus cavernosum of penis in ED rats, we used immunofluorescence assay to determine the expression of platelet and endothelial cell adhesion molecule 1 (PECAM-1) and eNOS in corpus cavernosum of penis (Fig. 6D). The results ((Fig. 6E) showed that compared to the normal group, PECAM-1 and eNOS expression was significantly lower in the ED group (all $p < 0.05$). Compared with the ED group, PECAM-1 and eNOS expression did not differ in the si-NC group and the mimic-NC group (all $p > 0.05$). In the si-lncRNA-MIAT group, PECAM-1 and eNOS expression was significantly increased compared with the si-NC group (all $p < 0.05$). In the miR-328a-5p mimic group, PECAM-1 and eNOS expression was significantly increased compared with the mimic-NC group (all $p < 0.05$). PECAM-1 and eNOS expression was significantly reduced in the miR-328a-5p

Table 3
Serum levels of ROS, NO and GSH after treatment with overexpression of lncRNA-MIAT and LPL.

	NC	oe-Lnc-MIAT	oe-LPL	oe-Lnc-MIAT + oe-LPL
ROS (U/mL)	161.56 ± 10.66	201.12 ± 10.10*	210.13 ± 11.84*	271.43 ± 13.43#
NO (uM)	95.41 ± 6.43	80.17 ± 5.68*	78.41 ± 5.01*	62.81 ± 5.03#
GSH (nmol/mg protein)	60.12 ± 6.84	48.43 ± 3.41*	45.15 ± 3.13*	32.14 ± 1.45#

Note: ROS, reactive oxygen species; NO, nitric oxide; GSH, glutathione; HG, high glucose; LPL, lipoprotein lipase; lncRNA-MIAT, long non-coding RNA myocardial infarction associated transcript; NC, negative control; $^{*}p < 0.05$, *vs.* the NC group; $^{\#}p < 0.05$, *vs.* the oe-lncRNA-MIAT and oe-LPL groups; the measurement data were expressed as mean ± standard deviation and data among multiple groups were compared with one-way analysis of variance; the experiment was repeated 3 times.

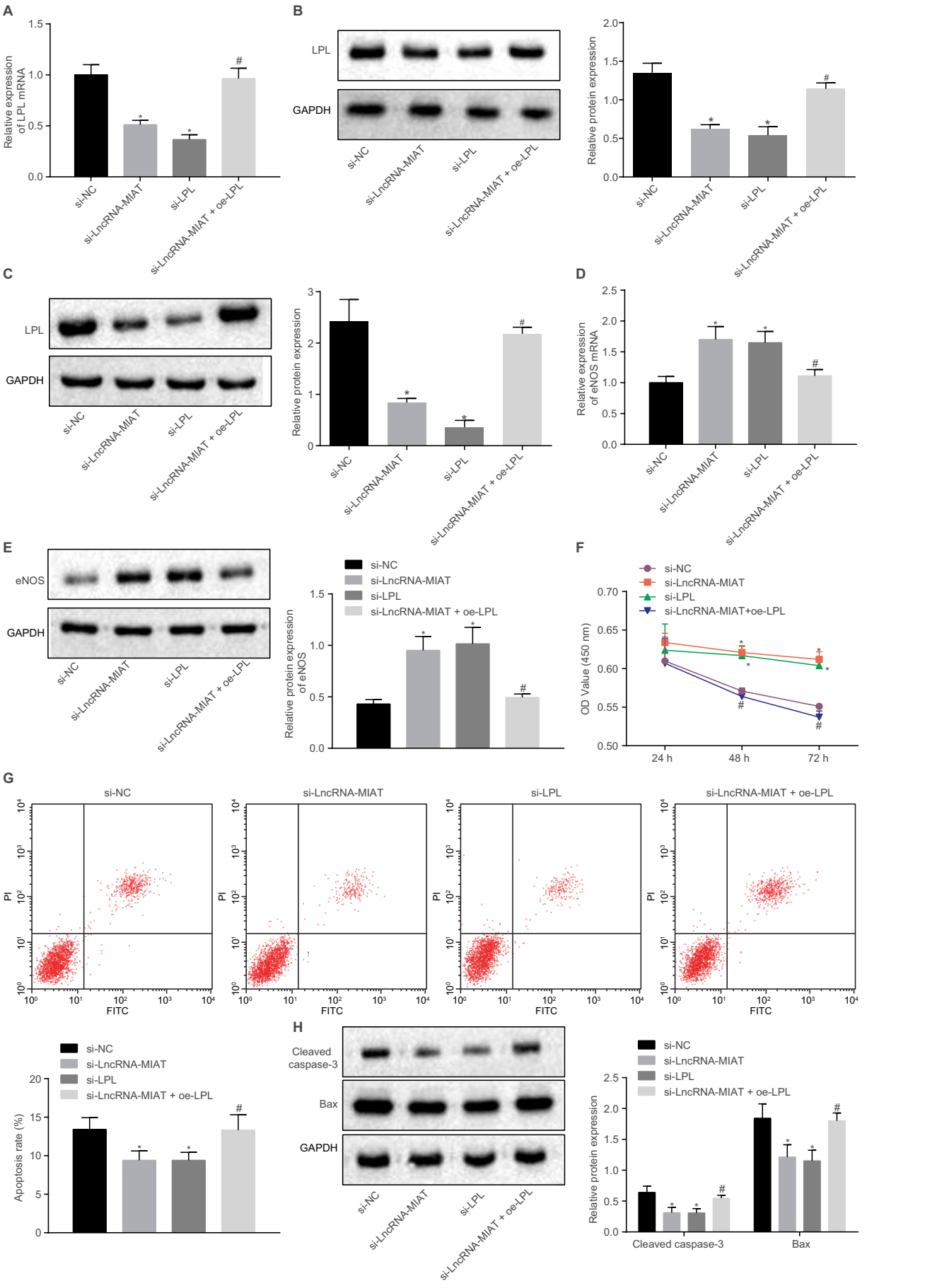

(caption on next page)

Fig. 4. Knockdown of lncRNA-MIAT or LPL prevents VEC injury induced by high glucose. A, qRT-PCR revealed that knockdown of lncRNA-MIAT or LPL decreased LPL mRNA levels in smooth muscle; B, western blot analysis demonstrated that LPL protein levels decreased in smooth muscle after si-lncRNA-MIAT or si-LPL treatment; C, western blot analysis demonstrated that LPL protein levels decreased in VECs after si-lncRNA-MIAT or si-LPL treatment; D, qRT-PCR revealed that eNOS mRNA levels increased in VECs after si-lncRNA-MIAT or si-LPL treatment; E, western blot analysis demonstrated that eNOS protein levels increased in VECs after si-lncRNA-MIAT or si-LPL treatment; F, knockdown of lncRNA-MIAT or LPL increased VEC proliferation as measured by CCK-8 assay; G, knockdown of lncRNA-MIAT or LPL decreased VEC apoptosis rate as measured by flow cytometry; Panel H, knockdown of lncRNA-MIAT or LPL decreased cleaved caspase-3 and Bax protein level as detected by western blot analysis; $^{*}p < 0.05$, *vs*. the si-NC group; $\#p < 0.05$, *vs*. the si-lncRNA-MIAT group; the measurement data were expressed as the mean ± standard deviation, comparisons among multiple groups were analyzed by one-way analysis of variance; data in Panel F were analyzed using two-way analysis of variance; the experiment was repeated thrice; lncRNA-MIAT, long noncoding RNA myocardial infarction associated transcript; LPL, lipoprotein lipase; miR-328a-5p, microRNA-328a-5p; ED, erectile dysfunction; NC, negative control; GAPDH, glyceraldehyde-3-phosphate dehydrogenase; VEC, vascular endothelial cells; qRT-PCR, reverse-transcription quantitative polymerase chain reaction; CCK-8, cell counting kit-8.

mimic + oe-LPL group compared with the miR-328a-5p mimic group (all $p < 0.05$). The above findings revealed that knockdown of lncRNA-MIAT or overexpression of miR-328a-5p could obviously promote VEC content and increase the expression of eNOS in VECs.

3. Discussion

As a major cause of ED and endothelial dysfunction, which are also known as vascular endothelial dysfunction, diabetes is identified as a risk factor for ED [15]. A previous study on ED revealed that this disorder can lead to reduced relaxant capacity, damaged vasodilation and reduced cGMP content in penile tissue [16], highlighting an unmet need for improving protective treatment in patients with ED. According to the microarray analysis, LPL is expressed highly in diabetics with ED, and bioinformatics prediction revealed that lncRNA-MIAT competitively bound to miR-328a-5p *via* mediating LPL. In addition, lncRNA-MIAT and LPL expression was increased in the serum of diabetic patients compared with healthy individuals, suggesting that LPL is highly expressed in diabetics. However, a rare study has reported the relationship between LPL and ED. In addition, a previous study reported that LPL is highly expressed in diabetic penile tissues, and high LPL expression increases the progression of ED [13]. To achieve that purpose, we established ED rat models and enrolled ED patients to investigate the mechanisms of lncRNA-MIAT/miR-328a-5p/LPL in VSMCs and VECs of diabetic rats and serum of patients. From our data, we observed that lncRNA-MIAT downregulation plays a potent protective role against ED *via* miR-328a-5p by suppressing LPL expression.

According to our results, miR-328a-5p was poorly expressed in VSMCs of diabetic rats, whereas LPL and lncRNA-MIAT were highly expressed. The expression of miR-328a-5p in serum of diabetic patients was downregulated in serum from diabetic patients. Moreover, online software analysis indicated that LPL was targeted and inhibited by miR-328a-5p. LncRNA-MIAT, which was recently found to be expressed in various diseases, such as myocardial infarction, schizophrenia, ischemic stroke, diabetic complications, age-related cataract and cancers, is a novel disease-related lncRNA [17]. LncRNA-MIAT is expressed at a significantly high level during angiogenesis, and its negative interaction with miR-150-5p upregulates the level of vascular endothelial growth factor (VEGC), therefore regulating endothelial cell function *via* a lncRNA-MIAT-miR-150-5p-VEGF feedback loop [18]. In addition, lncRNA-MIAT knockdown obviously alleviates diabetes-induced retinal microvascular dysfunction *in vivo* by disrupting endothelial cell proliferation, migration and tube formation [7]. Furthermore, our results revealed that lncRNA-MIAT was a competing endogenous RNA of miR-328a-5p and directly targeting miR-328a-5p. As a tumor suppressor, miR-328 is involved in the aggressive progression of various diseases, such as gliomas, colorectal cancer, and esophageal cancer [19–21]. A previous study revealed different expression of miR-328 in 3 types of diabetes [22]. In addition, another study also confirmed that miR-328 overexpression alleviated impairment of brown adipose tissue (BAT) by inhibiting Bace1, which can be used in the treatment of type 2 diabetes [9]. In addition, we found that LPL is a putative target gene of miR-328a-5p based on evidence from the online analysis software www.microrna.org. In type 2 diabetes, LPL mRNA and protein levels were increased, and its knockdown in muscle cells reduced mitochondrial levels by effectively reducing fatty acid delivery and subsequent activation of peroxisome proliferator-activated receptor (PPAR)-δ [12].

LncRNA-MIAT/LPL can cause VEC injury and apoptosis (NO and GSH serum levels and eNOS expression were reduced; ROS levels as well as cleaved caspase-3 and Bax expression were increased). In addition, inhibition of lncRNA-MIAT or upregulation of miR-328a-5p alleviated ED in diabetic rats. eNOS plays a critical role in the regulation of endothelial function through production of NO [23], which is a potent anti-apoptotic and cardioprotective molecule in healthy animals [24]. Some data from *in vitro* studies revealed that high-glucose medium disrupts eNOS expression in cultured endothelial cells [23]. In addition, in patients with DN, increased eNOS may be an effective strategy in restoring endothelial function [25]. Patients suffering from type 2 diabetes present severe insufficient GSH synthesis. This condition can be restored by dietary supplementation with GSH precursor amino acids, thus lowering oxidative stress and oxidant damage against persistent hyperglycemia [26]. In addition, increased ROS levels in mitochondria have been confirmed as the pathogenic cause for chronic complications of diabetes [27]. Bax is a nuclear-encoded protein involved in higher eukaryotes that is capable of piercing the mitochondrial outer membrane to mediate cell death by apoptosis, and a significant increase in Bax was noted in diabetic patients [28,29]. Furthermore, a study emphasized that suppression of lncRNA-MIAT inhibited apoptosis in cardiomyocytes cultured with high glucose [30]. Altogether, lncRNA-MIAT/LPL may be attributed to VEC injury and apoptosis.

In conclusion, our study demonstrates that lncRNA-MIAT silencing functions as a suppressor of ED progression. siRNA mediated silencing of lncRNA-MIAT led to downregulation of LPL expression *via* upregulating miR-328a-5p expression, thereby preventing VEC injury in VSMCs of the penis in the corpus cavernosum of diabetic rats with ED

Table 4
Serum levels of ROS, NO and GSH after lncRNA-MIAT and LPL inhibition.

	si-NC	si-Lnc-MIAT	si-LPL	si-Lnc-MIAT + oe-LPL
ROS (U/mL)	276.33 ± 25.65	165.56 ± 16.20*	160.43 ± 13.45*	238.09 ± 28.64#
NO (uM)	65.41 ± 5.41	87.01 ± 6.64*	87.21 ± 6.11*	70.15 ± 7.13#
GSH (nmol/mg protein)	29.32 ± 3.53	45.41 ± 5.01*	45.13 ± 4.13*	34.54 ± 1.74#

Note: ROS, reactive oxygen species; NO, nitric oxide; GSH, glutathione; HG, high glucose; NC, negative control; $^{*}p < 0.05$, *vs*. the si-NC group; $^{\#}p < 0.05$, *vs*. the si-lncRNA-MIAT groups; the measurement data were expressed as mean ± standard deviation, and data aming multiple groups were compared with one-way analysis of variance; the experiment was repeated 3 time.

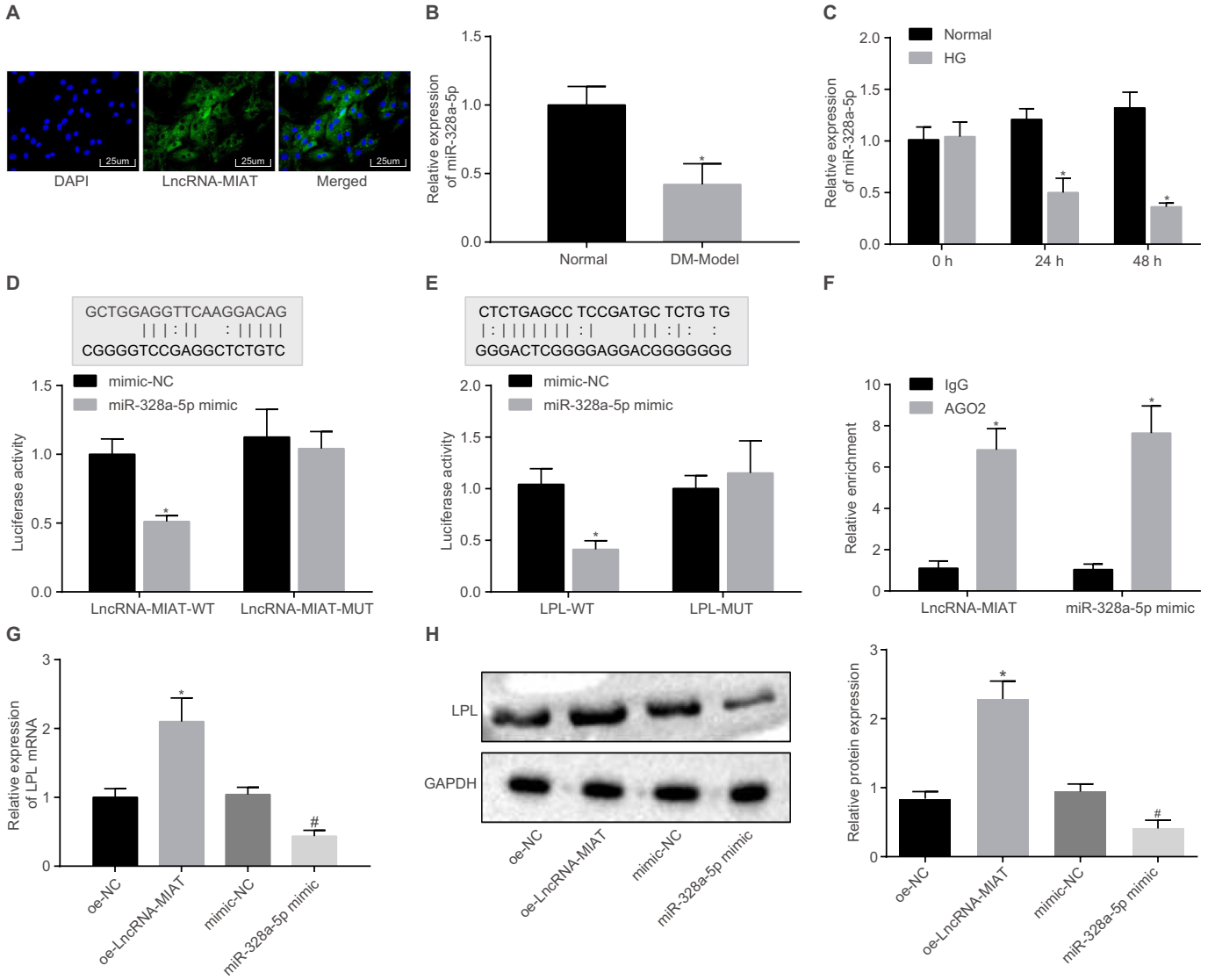

Fig. 5. LncRNA-MIAT positively regulates LPL expression by acting as a ceRNA of miR-328a-5p. A, lncRNA-MIAT is located in the cytoplasm (× 400, scale bar = 25 um); green represents lncRNA-MIAT, and blue represents the nucleus; B, miR-328a-5p expression was reduced in VSMCs in diabetic rats compared with normal rats as detected by qRT-PCR; *$p < 0.05$, *vs*. the normal rats; C, miR-328a-5p expression was increased in VSMCs cultured in normal medium compared with VSMCs cultured in high-glucose medium; *$p < 0.05$, *vs*. normal medium; D, lncRNA-MIAT directly targeted miR-328a-5p as detected using dual-luciferase reporter gene assay; *$p < 0.05$, *vs*. the mimic-NC group; E, LPL was directly targeted by miR-328a-5p as verified by dual-luciferase reporter gene assay; *$p < 0.05$, *vs*. the mimic-NC group; F, lncRNA-MIAT bound to AGO2 protein and targets miR-328a-5p as evaluated by RIP; *$p < 0.05$, *vs*. the IgG group; G, qRT-PCR revealed increased LPL mRNA level in VSMCs after lncRNA-MIAT and miR-328a-5p overexpression treatment; *$p < 0.05$, *vs*. the oe-NC group; #$p < 0.05$, *vs*. the mimic-NC group; H, western blot analysis demonstrated that LPL protein levels in VSMCs increased after lncRNA-MIAT and miR-328a-5p overexpression treatment; *$p < 0.05$, *vs*. the oe-NC group; #$p < 0.05$, *vs*. the mimic-NC group; the measurement data were expressed as the mean ± standard deviation, and comparisons among multiple groups were analyzed by one-way analysis of variance; the experiment was repeated thrice; lncRNA-MIAT, long noncoding RNA myocardial infarction associated transcript; LPL, lipoprotein lipase; miR-328a-5p, microRNA-328a-5p; ED, erectile dysfunction; Wt, wild type; Mut, mutant type; NC, negative control; VSMCs, vascular smooth muscle cells; qRT-PCR, reverse-transcription quantitative polymerase chain reaction; GAPDH, glyceraldehyde-3-phosphate dehydrogenase.

(Fig. 7). Therefore, the lncRNA-MIAT/miR-328a-5p/LPL axis could represent a potential biomarker for the treatment of ED in diabetes. Due to the complex mechanisms of diabetic ED and the numerous factors involved, the exact mechanisms underlying diabetic ED require further studies in the future.

4. Materials and methods

4.1. Ethics statement

The Ethics Committee of China-Japan Union Hospital of Jilin University approved the study. All animal experiments were performed in accordance with the Guide for the Care and Use of Laboratory Animal by International Committees [31]. Written informed consent was obtained from all participating patients (Clinical trial: ChiCTR1800019241. Registration time: 2018/11/1).

4.2. Bioinformatics prediction

Gene expression matrix and annotated probe files of chip data (GSE2457) related to ED were downloaded from the Gene Expression Omnibus (GEO) database (http://www.ncbi.nlm.nih.gov/geo), a sub-database of the National Center for Biotechnology Information (NCBI) (https://www.ncbi.nlm.nih.gov/). The data were obtained by detection

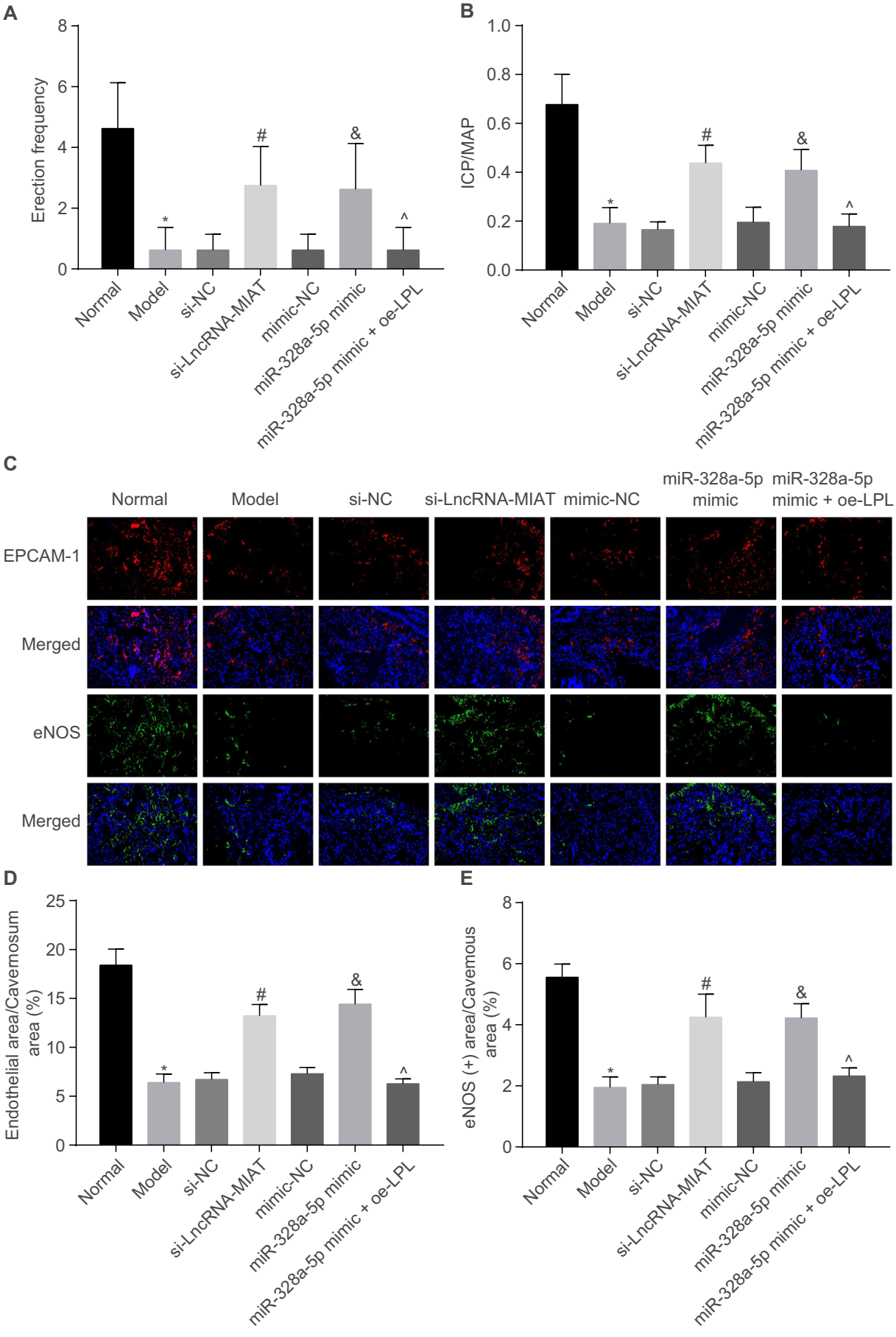

(caption on next page)

Fig. 6. Inhibition of lncRNA-MIAT or upregulation of miR-328a-5p improves ED in diabetic rats. A, lncRNA-MIAT silencing or miR-328a-5p overexpression increased erectile frequency in diabetic rats; B, lncRNA-MIAT silencing or miR-328a-5p overexpression increased ICP/MAP in the corpus cavernosum of penis in diabetic rats; C, PECAM-1 and eNOS protein levels in VECs in cavernous tissues (× 400, scale bar = 25 um); D, lncRNA-MIAT silencing or miR-328a-5p overexpression increased PECAM-1-positive cells in VECs; E, lncRNA-MIAT silencing or miR-328a-5p overexpression increased eNOS expression in VECs; *$p < 0.05$, *vs*. the control group; #$p < 0.05$, *vs*. the si-NC group; &$p < 0.05$, *vs*. the mimic-NC group; Λ$p < 0.05$, *vs*. the miR-328a-5p mimic group; measurement data were expressed as the mean ± standard deviation, and comparisons among multiple groups were analyzed by one-way analysis of variance; $n = 8$ (Panel A and Panel B); the experiment in Panel C~E was repeated thrice; lncRNA-MIAT, long noncoding RNA myocardial infarction associated transcript; LPL, lipoprotein lipase; miR-328a-5p, microRNA-328a-5p; ED, erectile dysfunction; NC, negative control; GAPDH, glyceraldehyde-3-phosphate dehydrogenase; ICP, intracavernosal pressure; MAP, mean arterial pressure; VEC, vascular endothelial cells; PECAM-1, platelet and endothelial cell adhesion molecule 1; eNOS, endothelial nitric-oxide synthase.

using GPL341-[RAE230A] Affymetrix Rat Expression 230A Array. "Affy" package of R software was employed for background correction and normalization preprocessing of each chip data [32], and "limma" package was used for screening DEGs [33]. Genes meeting the criteria (*p-Value* < 0.05 and |LogFoldChange| > 2 linear) were identified as the DEGs related with diabetic ED and were used to generate a heat map. The DEGs for further experiments were selected based on the interaction between proteins [34] obtained from String database (https://string-db.org/), and protein-protein interaction (PPI) network of DEGs was obtained using Cytoscape 3.6.0 software [35]. Finally, miRWalk (http://mirwalk.umm.uni-heidelberg.de/) was used to predict the miRNA that targets the DEGs, and the binding of lncRNA-miRNA was predicted by RNA22 (https://cm.jefferson.edu/rna22/).

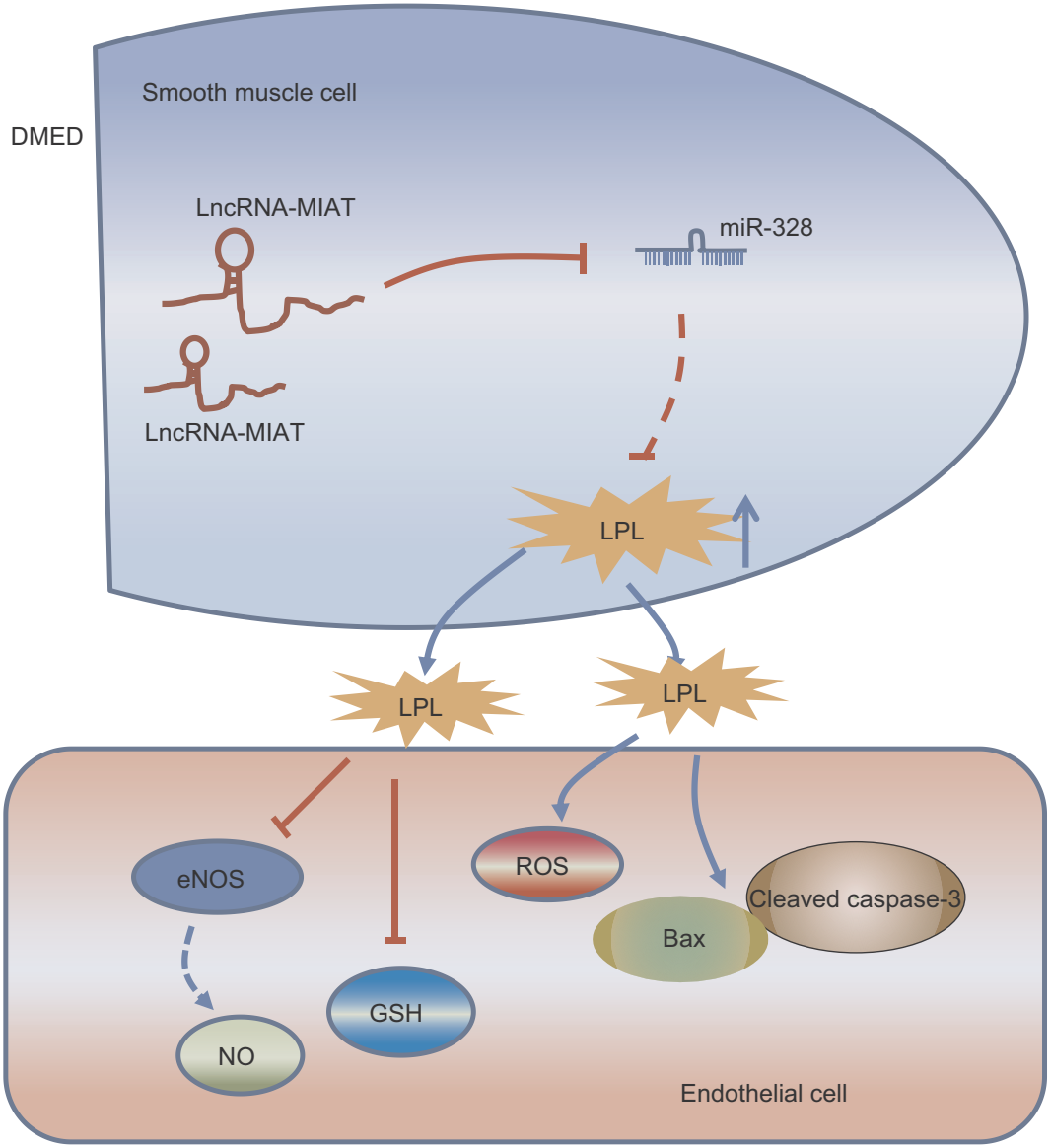

Fig. 7. Mechanism of lncRNA MIAT/miR-328a-5p/LPL axis in VEC injury and diabetic ED. LncRNA-MIAT in VSMCs of the penis in the corpus cavernosum combined with miR-328a-5p to upregulate LPL, contributing to VEC injury. NO and GSH serum levels and eNOS expression were disrupted, whereas ROS levels along with Bax and cleaved-caspase-3 expression were increased; lncRNA-MIAT, long noncoding RNA myocardial infarction associated transcript; LPL, lipoprotein lipase; miR-328a-5p, microRNA-328a-5p; ED, erectile dysfunction; ROS, reactive oxygen species; NO, nitric oxide; GSH, glutathione; Bax, Bcl2-associated X protein; VSMCs, vascular smooth muscle cells; VEC, vascular endothelial cells; eNOS, endothelial nitric-oxide synthase.

4.3. Study subjects

A total of 58 male patients (mean age: 52.62 ± 10.34) with diabetes hospitalized in China-Japan Union Hospital of Jilin University from 2015 to 2017 were enrolled in this study. All 58 type 2 diabetic patients were suffering from ED based on the 5-item version of the International Index of Erectile Function (IIEF-5), ultrasound parameters of the color of penis and exclusion criteria. None of these patients had any known thyroid dysfunction; hormone deficiency; genital malformation; Peyronie's disease and other sexual dysfunctions, including premature ejaculation or loss of sexual desire; history of pelvic surgery; renal and liver failure; and use of known drugs, such as antiandrogen, antihypertensive, antiarrhythmic, psychotropic drugs and antidepressants. The other 45 male patients with T2D without ED (mean age: 53.01 ± 10.34) and 40 age-matched healthy male volunteers (mean age: 52.03 ± 10.75) without sexual dysfunctions, diabetes or nervous system disease also participated in this study. The sera of these subjects were collected for further detection.

4.4. Rat model construction

A total of 68 male Sprague-Dawley (SD) rats (aging 10 weeks, weighing 280–300 g) were randomly grouped into STZ group ($n = 60$) and control group ($n = 8$). After 1 week of adaptive feeding and fasting for 12 h, STZ solution (STZ dissolved in 0.1 mol/L pH 4.0 citric acid-sodium citrate buffer solution, Sigma-Aldrich Chemical Company, St Louis, MO, USA) was intraperitoneally injected into rats at a dose of 60 mg/kg to generate the STZ rat model. The rats in the control group were treated with the same procedures as mentioned above and injected with the same amount of citric acid-sodium citrate buffer solution. The diabetic rats with ED were screened using APO. In total, 48 ED rats were successfully established and were then divided into 6 groups: ED group (ED rats without any transfection), si-NC group (ED rats transfected with siRNA NC sequences), si-lncRNA-MIAT group (ED rats transfected with si-lncRNA-MIAT sequences), mimic-NC group (ED rats transfected with ED rats transfected with miR-328a-5p mimic negative sequences), miR-328a-5p mimic group (ED rats transfected with miR-328a-5p mimic sequences), and miR-328a-5p mimic + oe-LPL group (ED rats transfected with miR-328a-5p mimic and oe-LPL sequences). Caudal vein injection procedures were performed as follows. Rats were fixed using a fixator on sterilized testing bed, and the tail of which was scrubbed repeatedly using alcohol. After dilation of rat tail veins, vectors and 25 μL lipofectamine 2000 were extracted with injection needle. Then, the proximal tail was processed with venous puncture using a 30-degree oblique view after removing the residual bubbles in the needle tube.

4.5. Apomorphine test

Eight weeks after the diabetic rat model was induced, the rats were treated with injection of APO (80 g/kg, dissolved in 0.9% saline solution and 0.2 g/L ascorbic acid) in the scruff of the neck and placed in an experimental cage. Next, the rats were observed by two individuals until erectile response occurred. When the hyperemia was found in the glans and the end of the penis, it was noted as an erection. Then, the yawn was counted when breathing with an obviously big mouth and apparent respiration movement were observed. Rats with a blood glucose level > 16.6 mM and without erectile reaction to APO were regarded as a successful diabetic ED model [36].

4.6. Detection of ICP and MAP

All grouped rats were subjected to ICP and MAP detection. Before detection, rats were treated with intraperitoneal anesthesia using 1% pentobarbital sodium (60–90 mg/kg, Sigma-Aldrich Chemical Company, St Louis, MO, USA). The penis was isolated through cutting the skin along the dorsum of the penis to the pubic symphysis. Then, the abdominal cavity was exposed along the ventral midline, and the major pelvic ganglion (MPG) at the posterolateral part of the prostate was considered as an electrical stimulation site. Subsequently, a 22-G needle with heparin salt water was used to puncture corpora cavernosum with connected pressure transducer for ICP recording, and the conducted left carotid artery intubation was subjected to continuous recording of MAP. After detectors were set, electrical stimulation was applied to MPG (rats received electrical stimulation of the cavernous nerve at a frequency of 15 Hz and a pulse width of 1.2 s for 1 min with a rest period of 2–3 min at 5 V) [37]. Changes of ICP/MAP were recorded using an RM6240 biological signal collection and disposal system (Chengdu Instrument Factory, Chengdu, China). After ICP/MAP measurement, rats were executed. The corpus cavernosum of penis was incised, flash-frozen using liquid nitrogen and then stored at −80 °C for further detection of related genes and proteins. ICP/MAP measurements were repeated thrice to obtain the average values.

4.7. Construction of lentivirus vectors

Lentivirus was used to overexpress and silence lncRNA-MIAT and LPL, respectively, and to overexpression miR-328a-5p. The full-length sequences of lncRNA-MIAT cDNA and LPL with restriction enzyme sites *Kpn*I and *Xho*I and shRNA sequences (designed by Thermo Fisher website) were synthesized. Synthesized sequences were cloned into lentivirus vector pLVX-IRES-neo using T4 ligase and then imported into *Escherichia coli*. Following amplification at 37 °C for 24 h, the plasmids were extracted. The final step of lncRNA-MIAT, LPL and their shRNA vector construction was to purify the destination vector and verify their sequences. Cells at 70%~80% confluence were used for transfection. Specifically, 12.5 μg of packed plasmids and 9 μL liposome were diluted in 250 μL serum-free RPMI1640 medium without penicillin/streptomycin, separately. After incubation at room temperature for 5 min, plasmid-RPMI1640 and liposome-RPMI1640 mixtures were mixed gently and incubated at room temperature for 20 min to form the plasmid-liposome complexes. Then, 293 T cell medium, which was placed in a 6-well plate and was used later for transfection, was replaced with serum-free RPMI1640 medium without penicillin/streptomycin. Subsequently, plasmid-liposome complexes were added to the 293 T cells followed by mixing and incubation at 37 °C for 6–8 h before inoculating the transfected cell culture with the complete medium. After transfection for 48–72 h, the cell suspension was centrifuged at 716 × *g* for 20 min to collect the lentivirus-rich supernatant, which was subsequently filtered through a 0.45-μm-pore-size filter to obtain virus concentrate with high concentration, and stored at −80 °C until use.

4.8. Cell treatment

The corpus cavernosum of the penis was isolated with the removal of cartilage of penis, lateral vascular tissue and peripheral fibrous adipose tissue in sterile conditions. Then, samples were washed several times in phosphate buffer saline (PBS). Subsequently, the tissues were cut into approximately 1- to 2-mm^3 tissue blocks, treated with 0.5% collagenase at 37 °C for 4 h, and then incubated in Dulbecco's Modified Eagle's Medium (DMEM, 100 U/mL penicillin and 100 U/mL streptomycin) containing 20% fetal bovine serum (FBS) in a 25-cm^2 culture bottle. After 3 days of incubation, cells could be seen growing from blocks, and the blocks were discarded on the following day. When cells reached 80% confluence, subculture was conducted to obtain 3rd generation or 4th generation cells. α-SMA-positive cells that were identified using immunofluorescence assay were considered primary VSMCs.

Cells were rinsed twice with serum-free Opti-MEM and then resuspended with 1.5 mL Opti-MEM. To prepare the vectors, 1 μg overexpressed vectors were added to 250 μL plasmid-containing Opti-MEM, which contained 3 μg siRNA plasmids or 3 μg NC plasmids. Then, 10 μL

lipofectamine 2000 were diluted in another 250 μL Opti-MEM and incubated at room temperature for 5 min. The diluted plasmids and lipofectamine 2000 were mixed gently and incubated at room temperature for 20 min to prepare plasmid-lipofectamine complex. Then, 500 μL of which was subsequently added to the cell suspension. After incubating the cell culture in 5% CO_2 at 37 °C for 6 h, the incubation medium was changed to complete culture medium. Then, the cell cultures were incubated overnight again in 5% CO_2 at 37 °C. On the next day, cell transfection was observed at 488 nm under a fluorescence microscope. When the transfection rate in each group was > 80%, three clusters were built, and 4 groups were present in each cluster. First, one-third of the cells were grouped into NC group, oe-lncRNA-MIAT group, oe-LPL group and oe-lncRNA-MIAT + oe-LPL group. Next, one-third of the cells were split into the si-NC group, si-lncRNA-MIAT group, si-LPL group and si-lncRNA-MIAT + oe-LPL group. Finally, the remaining cells were divided into NC group, oe-lncRNA-MIAT group, mimic-NC group and miR-328a-5p mimic group.

Then, 30-day-old rats were sacrificed and dissected in sterile conditions. The skin, muscles and diaphragm of the rats were cut open along the ventral midline to expose the chest, isolate abdomen, and cut aorta. After several washings, tunica adventitia of aorta and small branching vessels were removed. One end of the aorta was attached with a sterile silk thread and turned, causing the tunica adventitia to be exposed outward. The other end was quickly closed with sterile thread as well. Subsequently, the outward aorta was gently placed into a 25-cm^2 culture bottle pre-coated with Type I collagen from rat tail tendons, and DMEM containing 10% FBS was added to the bottle. Then, the bottle was placed into a cell culture box for incubation. When cells achieved 80% confluence, subculture was performed. The cells were subject to immunofluorescence assay, and PECAM-1-positive cells were considered as primary vessel cells.

The primary vessel cells were further cultured in the normal medium (5 mmol/L glucose), mannitol medium (30 mmol/L mannitol and normal medium with addition of 25 mmol/L mannitol) and high-glucose culture medium (30 mmol/L glucose, normal medium with addition of 25 mmol/L of glucose). The treated culture solution of VSMCs was collected as a conditioned medium and added to the culture medium of VEC.

4.9. ROS level determination

Dihydroethidium (DHE) staining in combination with flow cytometry was used to determine cellular ROS levels. Cell culture was incubated with 1 mM DHE at 37 °C for 15–25 min. After incubation with DHE, the cells were washed with PBS thrice, and DHE-treated cells were collected for ROS measurement.

4.10. NO content determination

NO content in cell culture supernatant was detected using colorimetry, and the determination of NO concentration was performed in accordance with the instructions of total nitrogen oxidase kit (Beyotime Biotechnology Co., Ltd., Shanghai, China).

4.11. GSH detection

The concentration of GSH was detected using the GSH kit (Sigma-Aldrich Chemical Company, St Louis, MO, USA). The cells were lysed, and the resulting lysate was mixed with equal volumes of 5% 5-sulfosalicylic for deproteinization. The supernatant was obtained by centrifugation at 4 °C at 17892 × *g* for 10 min. In a 96-well plate, 10 μL sample and 150 μL working fluid were added to each well followed by 5-min incubation at room temperature. The optical density (OD) was measured at a wavelength of 412 nm, and the final results were presented in nmol GSH/mg.

4.12. CCK-8 assay

Cell proliferation was measured based on the instructions of a CCK-8 kit (GM-040101-5, (Dojindo Molecular Technologies Inc., Gaithersburg, MD). Cells in each group were first washed with PBS, then treated with trypsin and finally resuspended after washing with PBS again. The resuspended cells were seeded into a 96-well plate at a density of 4×10^4 cells/μL with 6 duplicates for each group. After incubating the plate in a 5% CO_2 incubator at 37 °C for 2 d, 10 μL CCK-8 solution was added into each well of the plate. After incubation for 4 h, the OD value was measured using a spectrophotometer (UV-1800A, Shanghai Macy Instrument Co., Ltd., Shanghai, China) at a wavelength of 450 nm with 3 repetitions. OD value = $\text{OD value}_{\text{the experiment group}} - \text{OD value}_{\text{the blank group}}$.

4.13. Flow cytometry

Prior to measurement, cells were collected, treated with 0.25% trypsin, and adjusted to a density of 1×10^6 cells/mL. A total of 1 mL of cells was collected by centrifuging at 403 × *g* for 10 min to discard supernatant. After two washes with PBS, cells were centrifuged and resuspended in 200 μL binding buffer solution. Then, cells were mixed gently with 10 μL Annexin V-FITC and 5 μL PI and then reacted at room temperature for 15 min, avoiding light exposure. Then, 300 μL binding buffer solution was added to the cells, and cell apoptosis was detected using flow cytometry at an excitation wavelength of 488 nm.

4.14. Dual-luciferase reporter gene assay

The target gene analysis of miR-328a-5p was performed using the biological prediction website microRNA.org and verified using dual-luciferase reporter gene assays. The fragments of lncRNA-MIAT and LPL 3′UTR were synthesized and then introduced into pMIR-reporter (Huayueyang Biotechnology Co., Ltd., Beijing, China) using the restriction sites *Spe* I and Hind III. A complementary sequence mutation site of the seed sequence was designed based on the wild type (WT) sequences of lncRNA-MIAT and LPL. The target fragment was inserted into the pMIR-reporter plasmid using T4 DNA ligase after digestion with restriction endonuclease. The correct luciferase reporter plasmids of WT and mutant type (MUT) were co-transfected into HEK-293T cells (Bei Nuo Biotechnology Co., Ltd., Shanghai, China) with miR-328a-5p. Transfected cells were harvested and lysed at 48 h after transfection, and luciferase activity was measured according to luciferase assay kit (K801–200, Biovision, Mountain View, CA, USA) using Glomax20/20 luminometer fluorescence detection instrument (Promega, Madison, WI, USA). The experiment was repeated thrice.

4.15. Rip

A RIP kit (Millipore, Temecula, CA, USA) was used to evaluate the binding of lncRNA-MIAT and AGO2 proteins. Neurons were washed with precooled PBS, after which the supernatant was discarded. Cells were lysed with equal volume RIPA lysate (P0013B, Beyotime Biotechnology Co., Ltd., Shanghai, China) for 5 min in an ice bath followed by 10-min centrifugation at 4 °C at 35068 × *g* to obtain the supernatant. A small amount of supernatant was taken as the input, and the remaining was used for coprecipitation with antibodies. The experiment was performed as follows: 50 μL magnetic beads was extracted from each coprecipitation reaction system and resuspended in 100 μL RIP wash buffer after washing. Then, 5 μg AGO2 antibody (ab32381, 1:50, Abcam, Cambridge, MA, UK; mixed evenly for 30 min at room temperature) and IgG (1:100, ab109489, Abcam, Cambridge, MA, UK; as negative control) were added to the remaining supernatant of each group. Then, bead-antibody complexes were washed, resuspended in 900 μL RIP wash buffer with 100 μL cell extract, and incubated at 4 °C overnight. The samples were transferred on a pedestal to

collect bead-antibody protein complexes. When the samples and the input were treated with protease K, RNA was extracted for qRT-PCR detection.

4.16. Immunofluorescence assay

The corpus cavernosum of the penis was fixed in 4% neutral formaldehyde buffer (DF0113, Beijing Solarbio Science & Technology Co. Ltd., Beijing, China), embedded with paraffin, and cut into 4-μm serial sections. The sections were baked at 60 °C for 1 h, dewaxed with xylene (YB-5485, Shanghai Yu Bo Biological Technology Co., Ltd., Shanghai, China), hydrated with gradient alcohol, soaked in 3% H_2O_2 at room temperature for 20 min to eliminate the activity of endogenous peroxidase, and washed with PBS. After drying, the sections were treated with heat antigen retrieval twice and then blocked with 10% goat serum for 15 min. The sections were then reacted with the immunofluorescence primary antibody PECAM-1 (ab28364, 1:20, Abcam Inc., Cambridge, MA, USA) and eNOS (ab5589, 1:50, Abcam Inc., Cambridge, MA, USA), and washed with PBS thrice for 5 min each time. Next, sections were incubated with immunofluorescence secondary antibody (1:500) for 2 h at room temperature without light and washed thrice with PBS for 5 min each time. The sections were incubated with 4,6-diamidino-2-phenyl-indole (DAPI) (ab104139, 1:100, Abcam Company, Shanghai, China) for 10 min at room temperature without light and washed thrice with PBS for 5 min each time. At the end, sections were mounted with sealant and observed using an inverted microscope.

4.17. qRT-PCR

Total RNA was extracted using the ultra-pure RNA extraction kit (16,096,020, Thermo Fisher Scientific Inc., Waltham, MA, USA) according to the manufacturer's protocol. After RNA extraction, 5 μg RNA was reversely transcribed into the cDNA in accordance with the instructions of the qRT-PCR kit (Applied Biosystems Inc., Foster City, CA, USA). PCR amplification was conducted using a 25-μL PCR reaction system, which included 300 ng cDNA, 1 × PCR buffer, 200 μmol/L of dNTP, 80 pmol/L forward primer, 80 pmol/L reverse primer, and 0.5 U Taq-enzyme (S10118, Shanghai, Yuan Ye Biotechnology Co., Ltd., Shanghai, China). The reaction conditions consisted of predenaturation at 94 °C for 5 min; 30 cycles of denaturation at 94 °C for 30 s, annealing at 54.5 °C for 30 s and extension at 72 °C for 30 s; and final extension at 72 °C for 10 min. The amplified products were stored at 4 °C before use. The primer sequences of lncRNA-MIAT, miR-328a-5p, lipoprotein lipase (LPL), endothelial nitric-oxide synthase (eNOS), U6 and glyceraldehyde-3-phosphate dehydrogenase (GAPDH) are presented in Table 4. The U6 gene was used as the internal reference of miR-328a-5p, whereas GAPDH served as the internal reference for lncRNA-MIAT, LPL and eNOS. Here, $2^{-\Delta\Delta Ct}$ represented the ratio of the expression of the target gene in the experiment group compared with the control group. The following formula was used: $\Delta\Delta CT = \Delta Ct_{\text{experimental group}} - \Delta Ct_{\text{control group}}$, where $\Delta Ct = Ct_{\text{target gene}} - Ct_{\text{internal reference}}$. Ct was the amplification cycles when the real-time fluorescence intensity of the reaction reached the set threshold, and the amplification was in the logarithmic growth. The experiment was independently repeated thrice.

4.18. Western blot analysis

Total protein was extracted from tissues and cells using RIPA lysate (R0010, Beijing Solarbio Science & Technology Co., Ltd., Beijing, China) containing phenylmethylsulfonyl fluoride (PMSF) on ice for 30 min and centrifuged at 25764 × *g* at 4 °C for 10 min with supernatant collected. The concentration of each protein extract (23,225, Pierce, Rockford, IL, USA) was determined using a bicinchoninic acid (BCA) kit and then adjusted with deionized water. A total of 10% sodium dodecyl sulfate-polyacrylamide gel (SDS-PAGE) (P0012A, Beyotime Institute of Biotechnology, Shanghai, China) was prepared. Then, 50 μg protein sample was loaded in each well followed by 2-h electrophoresis at a constant voltage of 80 V. The separated proteins were transferred to a polyvinylidene fluoride (PVDF) membrane (ISEQ00010, Millipore, Billerica, MA, USA) *via* a wet phase-inversion process at 110 V for 2 h. The membranes were blocked with Tris-buffered saline Tween-20 (TBST) containing 5% skim milk for 2 h, washed with TBST, and then incubated with the following primary antibodies at 4 °C overnight: eNOS (ab5589, 1:50, Abcam, Cambridge, MA, USA), LPL (1:1000, ab93898, Abcam, Cambridge, MA, UK), cleaved-caspase-3 (ab2302, 1:1000, Abcam, Cambridge, MA, USA), Bax (ab53154, 1:1000, Abcam, Cambridge, MA, USA) and GAPDH (1:2000, ab9485, Abcam, Cambridge, MA, UK). After three 10-min washes with TBST, the membranes were incubated with horseradish peroxidase (HRP)-labeled secondary antibody for 1 h and then washed with TBST before placing on clean glass plate. Then, an equal amount of solution A and solution B from the chemiluminescence (ECL) detection kit (BB-3501, Amersham Pharma-cia Biotech, Little Chalfont, UK) were mixed in the dark and then applied to the membranes, which were exposed and imaged onto gel imaging instrument. The membranes were photographed using Bio-Rad image analysis system (Bio-Rad Laboratories, Hercules, CA, USA) and analyzed using Quantity One v4.6.2 software. The relative protein concentration was presented as the ratio of gray value of protein bands and GAPDH protein bands. The experiment was repeated thrice.

4.19. Statistical analysis

SPSS 21.0 statistical software (IBM Corp., Armonk, NY, USA) was used to analyze data in our study. Measurement data were presented as the mean ± standard deviation. The measurement data were analyzed with the Kolmogorov-Smirnov test for normal distribution. Tukey's test for multiple comparisons of one-way analysis of variance was used to compare data with normal distribution among multiple groups for *post hoc* tests, and Dunn's multiple comparison of Kruskal-Wallis test was used to compare data with skewed distribution among multiple groups for *post hoc* test. Data with normal distribution and/or homogeneity of variance were compared using an unpaired *t*-test between two groups and using paired *t*-test in the same group. Data with homogeneity of variances were analyzed using Welch's *t*-test. Cell proliferation was analyzed using two-way analysis of variance. Count data were presented as percentage and compared with chi-square test. A p-value < 0.05 was considered to be statistically significant.

Author contributions

HW designed the study. HY and LH collated the data, designed and developed the database, performed data analyses and produced the initial draft of the manuscript. LY contributed to drafting the manuscript. All authors participated in the revised manuscript and have read and approved the final submitted manuscript.

Transparency document

The Transparency document associated this article can be found, in online version.

Acknowledgement

We acknowledge and appreciate our colleagues for their valuable efforts and comments on this paper.

Competing interests

The authors declare that they have no competing interests.

Funding

None.

Appendix A. Supplementary data

Supplementary data to this article can be found online at https://doi.org/10.1016/j.bbadis.2019.01.018.

References

[1] A. American Diabetes, Diagnosis and classification of diabetes mellitus, Diabetes Care 32 (Suppl. 1) (2009) S62–S67.
[2] J. Hidalgo-Tamola, K. Chitaley, Review type 2 diabetes mellitus and erectile dysfunction, J. Sex. Med. 6 (2009) 916–926.
[3] V.S. Thorve, A.D. Kshirsagar, N.S. Vyawahare, V.S. Joshi, K.G. Ingale, R.J. Mohite, Diabetes-induced erectile dysfunction: epidemiology, pathophysiology and management, J. Diabetes Complicat. 25 (2011) 129–136.
[4] I. Goldstein, L.A. Jones, L.H. Belkoff, G.S. Karlin, C.H. Bowden, C.A. Peterson, B.A. Trask, W.W. Day, Avanafil for the treatment of erectile dysfunction: a multicenter, randomized, double-blind study in men with diabetes mellitus, Mayo Clin. Proc. 87 (2012) 843–852.
[5] S. Cellek, N.E. Cameron, M.A. Cotter, A. Muneer, Pathophysiology of diabetic erectile dysfunction: potential contribution of vasa nervorum and advanced glycation endproducts, Int. J. Impot. Res. 25 (2013) 1–6.
[6] X.I. Jiang, Y. Luo, S. Zhao, Q. Chen, C. Jiang, Y. Dai, Y. Chen, Z. Cao, Clinical significance and expression of microRNA in diabetic patients with erectile dysfunction, Exp. Ther. Med. 10 (2015) 213–218.
[7] B. Yan, J. Yao, J.Y. Liu, X.M. Li, X.Q. Wang, Y.J. Li, Z.F. Tao, Y.C. Song, Q. Chen, Q. Jiang, lncRNA-MIAT regulates microvascular dysfunction by functioning as a competing endogenous RNA, Circ. Res. 116 (2015) 1143–1156.
[8] B.A. Hurschler, D.T. Harris, H. Grosshans, The type II poly(a)-binding protein PABP-2 genetically interacts with the let-7 miRNA and elicits heterochronic phenotypes in Caenorhabditis elegans, Nucleic Acids Res. 39 (2011) 5647–5657.
[9] M. Oliverio, E. Schmidt, J. Mauer, C. Baitzel, N. Hansmeier, S. Khani, S. Konieczka, M. Pradas-Juni, S. Brodesser, T.M. Van, D. Bartsch, H.S. Bronneke, M. Heine, H. Hilpert, E. Tarcitano, G.A. Garinis, P. Frommolt, J. Heeren, M.A. Mori, J.C. Bruning, J.W. Kornfeld, Dicer1-miR-328-Bace1 signalling controls brown adipose tissue differentiation and function, Nat. Cell Biol. 18 (2016) 328–336.
[10] Y. Bai, L. Zhang, Y. Jiang, J. Ju, G. Li, J. Xu, X. Jiang, P. Zhang, L. Lang, O. Sadkovaya, P.V. Glybochko, W. Zhang, B. Yang, Identification and functional verification of MicroRNAs in the obese rat with erectile dysfunction, Sex Med. 5 (2017) e261–e271.
[11] H. Wang, G. Astarita, M.D. Taussig, K.G. Bharadwaj, N.V. DiPatrizio, K.A. Nave, D. Piomelli, I.J. Goldberg, R.H. Eckel, Deficiency of lipoprotein lipase in neurons modifies the regulation of energy balance and leads to obesity, Cell Metab. 13 (2011) 105–113.
[12] K. Morino, K.F. Petersen, S. Sono, C.S. Choi, V.T. Samuel, A. Lin, A. Gallo, H. Zhao, A. Kashiwagi, I.J. Goldberg, H. Wang, R.H. Eckel, H. Maegawa, G.I. Shulman, Regulation of mitochondrial biogenesis by lipoprotein lipase in muscle of insulin-resistant offspring of parents with type 2 diabetes, Diabetes 61 (2012) 877–887.
[13] C.J. Sullivan, T.H. Teal, I.P. Luttrell, K.B. Tran, M.A. Peters, H. Wessells, Microarray analysis reveals novel gene expression changes associated with erectile dysfunction in diabetic rats, Physiol. Genomics 23 (2005) 192–205.
[14] J. Zhang, M. Chen, J. Chen, S. Lin, D. Cai, C. Chen, Z. Chen, Long non-coding RNA MIAT acts as a biomarker in diabetic retinopathy by absorbing miR-29b and regulating cell apoptosis, Biosci. Rep. 37 (2017).
[15] M.I. Maiorino, G. Bellastella, E. Della Volpe, O. Casciano, L. Scappaticcio, P. Cirillo, D. Giugliano, K. Esposito, Erectile dysfunction in young men with type 1 diabetes, Int. J. Impot. Res. 29 (2017) 17–22.
[16] J. Angulo, R. Gonzalez-Corrochano, P. Cuevas, A. Fernandez, J.M. La Fuente, F. Rolo, A. Allona, I. Saenz de Tejada, Diabetes exacerbates the functional deficiency of NO/cGMP pathway associated with erectile dysfunction in human corpus cavernosum and penile arteries, J. Sex. Med. 7 (2010) 758–768.
[17] C. Sun, L. Huang, Z. Li, K. Leng, Y. Xu, X. Jiang, Y. Cui, Long non-coding RNA MIAT in development and disease: a new player in an old game, J. Biomed. Sci. 25 (2018) 23.
[18] L. Jian, D. Jian, Q. Chen, L. Zhang, Long noncoding RNAs in atherosclerosis, J. Atheroscler. Thromb. 23 (2016) 376–384.
[19] Z. Wu, L. Sun, H. Wang, J. Yao, C. Jiang, W. Xu, Z. Yang, MiR-328 expression is decreased in high-grade gliomas and is associated with worse survival in primary glioblastoma, PLoS One 7 (2012) e47270.
[20] X.T. Xu, Q. Xu, J.L. Tong, M.M. Zhu, F. Nie, X. Chen, S.D. Xiao, Z.H. Ran, MicroRNA expression profiling identifies miR-328 regulates cancer stem cell-like SP cells in colorectal cancer, Br. J. Cancer 106 (2012) 1320–1330.
[21] N. Han, W. Zhao, Z. Zhang, P. Zheng, MiR-328 suppresses the survival of esophageal cancer cells by targeting PLCE1, Biochem. Biophys. Res. Commun. 470 (2016) 175–180.
[22] G. Alieh, A.T. Hossein, G.F. Mohammad, Identification of candidate microrna biomarkers in renal fibrosis: a meta-analysis of profiling studies, Biomarkers 23 (2018) 713–724.
[23] H. Cheng, H. Wang, X. Fan, P. Paueksakon, R.C. Harris, Improvement of endothelial nitric oxide synthase activity retards the progression of diabetic nephropathy in db/db mice, Kidney Int. 82 (2012) 1176–1183.
[24] Y. Liu, C. Xia, R. Wang, J. Zhang, T. Yin, Y. Ma, L. Tao, The opposite effects of nitric oxide donor, S-nitrosoglutathione, on myocardial ischaemia/reperfusion injury in diabetic and non-diabetic mice, Clin. Exp. Pharmacol. Physiol. 44 (2017) 854–861.
[25] Z.J. Ma, R. Chen, H.Z. Ren, X. Guo, J.G. Chen, L.M. Chen, E. Collaborative Innovation, Center of Tianjin for medical, endothelial nitric oxide synthase (eNOS) 4b/a polymorphism and the risk of diabetic nephropathy in type 2 diabetes mellitus: a meta-analysis, Meta Gene 2 (2014) 50–62.
[26] R.V. Sekhar, S.V. McKay, S.G. Patel, A.P. Guthikonda, V.T. Reddy, A. Balasubramanyam, F. Jahoor, Glutathione synthesis is diminished in patients with uncontrolled diabetes and restored by dietary supplementation with cysteine and glycine, Diabetes Care 34 (2011) 162–167.
[27] O. Savu, V.G. Sunkari, I.R. Botusan, J. Grunler, A. Nikoshkov, S.B. Catrina, Stability of mitochondrial DNA against reactive oxygen species (ROS) generated in diabetes, Diabetes Metab. Res. Rev. 27 (2011) 470–479.
[28] D. Westphal, G. Dewson, P.E. Czabotar, R.M. Kluck, Molecular biology of Bax and Bak activation and action, Biochim. Biophys. Acta 1813 (2011) 521–531.
[29] T. Khalfaoui, N. Basora, A. Ouertani-Meddeb, Apoptotic factors (Bcl-2 and Bax) and diabetic retinopathy in type 2 diabetes, J. Mol. Histol. 41 (2010) 143–152.
[30] X. Zhou, W. Zhang, M. Jin, J. Chen, W. Xu, X. Kong, lncRNA MIAT functions as a competing endogenous RNA to upregulate DAPK2 by sponging miR-22-3p in diabetic cardiomyopathy, Cell Death Dis. 8 (2017) e2929.
[31] J. Wang, Y. Mi, F. Yuan, S. Wu, X. You, F. Dai, Y. Huang, J. Cao, J. Zhu, B. Xue, L. Zhu, The involvement of corin in the progression of diabetic erectile dysfunction in a rat model by down-regulating ANP/NO/cGMP signal pathway, J. Cell. Biochem. 118 (2017) 2325–2332.
[32] L. Gautier, L. Cope, B.M. Bolstad, R.A. Irizarry, Affy–analysis of Affymetrix GeneChip data at the probe level, Bioinformatics 20 (2004) 307–315.
[33] G.K. Smyth, Linear models and empirical bayes methods for assessing differential expression in microarray experiments, Stat. Appl. Genet. Mol. Biol. 3 (2004) Article 3.
[34] D. Szklarczyk, A. Franceschini, S. Wyder, K. Forslund, D. Heller, J. Huerta-Cepas, M. Simonovic, A. Roth, A. Santos, K.P. Tsafou, M. Kuhn, P. Bork, L.J. Jensen, C. von Mering, STRING v10: protein-protein interaction networks, integrated over the tree of life, Nucleic Acids Res. 43 (2015) D447–D452.
[35] P. Shannon, A. Markiel, O. Ozier, N.S. Baliga, J.T. Wang, D. Ramage, N. Amin, B. Schwikowski, T. Ideker, Cytoscape: a software environment for integrated models of biomolecular interaction networks, Genome Res. 13 (2003) 2498–2504.
[36] J. Wang, Y. Mi, F. Yuan, S. Wu, X. You, F. Dai, Y. Huang, J. Cao, J. Zhu, B. Xue, L. Zhu, The involvement of corin in the progression of diabetic erectile dysfunction in a rat model by down-regulating ANP/NO/cGMP signal pathway, J. Cell. Biochem. 118 (2017) 2325–2332.
[37] H. Wang, X.G. Ding, J.J. Yang, S.W. Li, H. Zheng, C.H. Gu, Z.K. Jia, L. Li, LncRNA MIAT facilitated BM-MSCs differentiation into endothelial cells and restored erectile dysfunction via targeting miR-200a in a rat model of erectile dysfunction, Eur. J. Cell Biol. 97 (2018) 180–189.